Engineering of strong mechanical squeezing via the joint effect between Duffing nonlinearity and parametric pump driving

CHENG-HUA BAI,[1] DONG-YANG WANG,[1] SHOU ZHANG,[1,2,3] SHUTIAN LIU,[1] (iD) AND HONG-FU WANG[2,*]

[1]*Department of Physics, Harbin Institute of Technology, Harbin 150001, China*
[2]*Department of Physics, College of Science, Yanbian University, Yanji 133002, China*
[3]*e-mail: szhang@ybu.edu.cn*
Corresponding author: hfwang@ybu.edu.cn

Previous works for achieving mechanical squeezing focused mainly on the sole squeezing manipulation method. Here we study how to construct strong steady-state mechanical squeezing via the joint effect between Duffing nonlinearity and parametric pump driving. We find that the 3 dB limit of strong mechanical squeezing can be easily overcome from the joint effect of two different below 3 dB squeezing components induced by Duffing nonlinearity and parametric pump driving, respectively, without the need of any extra technologies, such as quantum measurement or quantum feedback. Especially, we first demonstrate that, in the ideal mechanical bath, the joint squeezing effect just is the superposition of the two respective independent squeezing components. The mechanical squeezing constructed by the joint effect is fairly robust against the mechanical thermal noise. Moreover, different from previous mechanical squeezing detection schemes, which need to introduce an additional ancillary cavity mode, the joint mechanical squeezing effect in the present scheme can be directly measured by homodyning the output field of the cavity with an appropriate phase. The joint idea opens up a new approach to construct strong mechanical squeezing and can be generalized to realize other strong macroscopic quantum effects.   © 2019 Chinese Laser Press

https://doi.org/10.1364/PRJ.7.001229

1. INTRODUCTION

The quantum fluctuations of a pair of quadrature observables, such as the amplitude and phase of the field, or the position and momentum of a mechanical oscillator, are bound by the Heisenberg uncertainty relation [1]. However, if the fluctuation of either of the two quadrature components is reduced below the standard quantum limit, it will be accompanied by increased fluctuation in the other quadrature. This is the so-called squeezed state. Since the squeezed state is particularly useful for improvement of the precision of quantum measurements at the quantum level [2–4], test of the quantum theory fundamentals [5], exploration of the borderline between quantum and classical [6,7], and also an important resource in quantum information science for continuous-variable information processing [8], achieving such a state has been actively pursued in the past decades.

In the realm of optics, the quantum squeezing of light has been observed in the 1980s [9–11]. However, due to the strong decoherence from undesired coupling with the environment, it has been a formidable challenge to obtain squeezing in the motional state of the macroscopic massive object. Although the squeezing in the oscillations of massive gravitational antennae was proposed a long time ago [12], the technological requirements are too severe for experimental realization. To our excitement, owing to the tremendous progress made in cavity optomechanics [13], such as the ground-state cooling of macroscopic mechanical oscillators [14–18] and the realization of strong optomechanical coupling [19–21], the optomechanical system provides a powerful tool for achieving the squeezed state of mechanical oscillators that are nearly macroscopic in physical size [22].

In recent years, a host of methods has been proposed to achieve mechanical squeezing based on the cavity optomechanical system, such as periodic modulation of the external driving amplitude [23–26], parametric driving of the mechanical oscillator [27], quantum reservoir engineering [28,29], squeezed light driving and squeezing transfer [30], quadratic optomechanical coupling [31,32], dissipative optomechanical coupling [33–35], Duffing nonlinearity [36], and parametric resonance induced by non-Markovian reservoir [37]. As we all know, if the quantum fluctuation of one of the mechanical quadratures

can be suppressed below one-half of the standard quantum limit, the squeezing of the mechanical oscillator beats the 3 dB limit, which has been the feature of achieving strong mechanical squeezing. However, in order to surpass this 3 dB limit, some schemes strongly depend on more complex technologies, including quantum measurements [38–40], quantum feedback [41], both linear and quadratic optomechanical couplings, and squeezed vacuum injection [42], etc. Additionally, the above-mentioned generation schemes of mechanical squeezing [23–34,36,37] focused mainly on the sole squeezing manipulation method. Thus, a novel idea is whether we can make use of the joint effect between two relatively simple squeezing methods to construct strong mechanical squeezing. If so, how the respective squeezing will affect the total squeezing effect needs investigation.

In this paper, we study the engineering of strong mechanical squeezing via the joint effect between Duffing nonlinearity and parametric pump driving. We find that, by properly choosing the parametric pump frequency, the squeezing of the cavity mode created by an optical parametric amplifier (OPA) can be further transferred into the squeezed mechanical mode induced by the Duffing nonlinearity. Based on this kind of joint squeezing effect, the beyond 3 dB strong mechanical squeezing can be easily achieved from two different below 3 dB squeezing components without the need of any extra technologies, such as quantum measurement or quantum feedback. We numerically and analytically show that, in the case of an ideal mechanical bath, the joint squeezing effect between Duffing nonlinearity and parametric pump driving just is the superposition of these two respective independent squeezing effects. The joint mechanical squeezing has significantly strong robustness against the mechanical thermal noise. Moreover, compared with previous mechanical squeezing detection schemes [36,37], there is no necessity to introduce an additional ancillary cavity mode in the present scheme, and the joint mechanical squeezing effect can be directly measured by homodyning the output field of the cavity. The idea of joint effect provides a new approach to generate strong mechanical squeezing and can also be generalized to realize other quantum effects, for example, enhancement of optomechanical entanglement via periodic modulations of the driving amplitude and the input laser intensity [43], optomechanical cooling beyond the quantum back-action limit with the frequency modulations of the cavity mode and the mechanical mode [44], and the realization of the ultrastrong Jaynes–Cummings mode by modulating the resonance frequencies of the two-level system and the bosonic mode [45].

The rest of this paper is structured as follows. In Section 2, we describe the physical mode and obtain the linearized system Hamiltonian. In Section 3, we analyze the stability of the system and calculate the steady-state quantum fluctuation spectra of the mechanical mode. In Section 4, we discuss in detail the joint effect between Duffing nonlinearity and parametric pump driving in the construction of strong mechanical squeezing from the points of squeezing transfer, Wigner function, and analytical result, respectively. In Section 5, we show how the joint squeezing effect can be measured by homodyning the output field of the cavity. In Section 6, we discuss experimental feasibility. Finally, we present our conclusions in Section 7.

2. MODEL AND HAMILTONIAN

We consider a degenerate OPA inside an optomechanical system formed by a fixed mirror and a moving mirror, as depicted in Fig. 1, in which the movable mirror is coupled to a single-mode cavity field (with frequency ω_c and decay rate κ) driven by an external laser field with amplitude ε_L and frequency ω_L. The fixed mirror is partially transmissive, while the movable mirror is completely reflective and is modeled as a quantum-mechanical oscillator with effective mass m, resonance frequency ω_m, damping rate γ_m, and Duffing nonlinearity amplitude η. As pointed out in Ref. [46], the mechanical nonlinearity can be generated by coupling the mechanical oscillator to an auxiliary system. It is shown that the strong nonlinearity of $\eta = 10^{-4}\omega_m$ can be obtained when the mechanical mode is coupled to a qubit [36]. Meanwhile, in the degenerate OPA, we assume that a pump field at frequency $2(\omega_L + \tilde{\omega}'_m)$ interacts with a second-order nonlinear optical crystal, and it generates downconverted light at frequency $\omega_L + \tilde{\omega}'_m$, the specific form of $\tilde{\omega}'_m$ of which will be given later. Moreover, the mechanical oscillator is also contacted with a thermal environment in equilibrium at temperature T, which induces a thermal Langevin force exerting on the mechanical oscillator. The Hamiltonian of the system in the rotating frame with respect to laser frequency ω_L is written as ($\hbar = 1$)

$$H = \delta_c c^\dagger c + \omega_m b^\dagger b + \frac{\eta}{2}(b + b^\dagger)^4 - g_0 c^\dagger c(b + b^\dagger)$$
$$+ \varepsilon_L(c^\dagger + c) + iG(e^{i\theta}c^{\dagger 2}e^{-2i\tilde{\omega}'_m t} - e^{-i\theta}c^2 e^{2i\tilde{\omega}'_m t}). \quad \text{(1)}$$

Here the first term is the energy of the cavity field, where $\delta_c = \omega_c - \omega_L$ is the cavity detuning with respect to the frequency of the input laser, and c ($c^\dagger$) refers to the annihilation (creation) operator of the cavity field satisfying the commutation relation $[c, c^\dagger] = 1$. The second and third terms correspond to the energy of the mechanical oscillator, which contain a Duffing nonlinearity term, and b ($b^\dagger$) is the annihilation (creation) operator of the mechanical mode, satisfying $[b, b^\dagger] = 1$. The fourth and fifth terms describe the interactions of the cavity field with the mechanical mode and the input laser, respectively, where g_0 is the single-photon optomechanical coupling strength. The last term represents the coupling between the cavity field and the OPA, where the gain of the
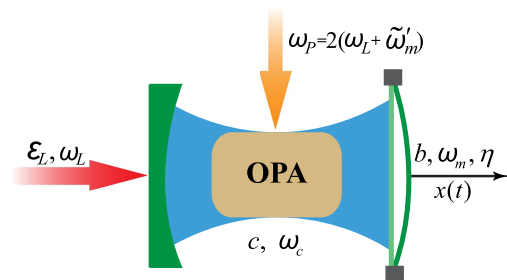
Fig. 1. Schematic diagram of the considered optomechanical system. An OPA is placed inside the cavity driven by an external laser field and is pumped by a parametric driving field. Here the movable mirror is coupled to the cavity field via the radiation-pressure interaction and is treated as a quantum-mechanical oscillator with a Duffing nonlinearity.

OPA is G, related to the power of the pump driving the OPA, and the phase of the pump driving the OPA is θ.

Here we are interested in the strong-driving regime so that both the cavity and the mechanical modes will be in the large steady-state amplitudes. Let α and β be the steady-state amplitude of the cavity mode and the mechanical mode under the strong-driving regime, respectively. We can obtain the following set of equations for the steady-state amplitudes:

$$[-i(\delta_c - 2g_0\beta) - \kappa]\alpha - i\varepsilon_L = 0,$$
$$16\eta\beta^3 + (12\eta + \omega_m)\beta - g_0|\alpha|^2 = 0, \tag{2}$$

where the G-dependent and γ_m-dependent terms have been omitted under the parameter regimes of $G \ll \omega_m$ and $\gamma_m \ll \kappa$.

Using the Heisenberg equations of motion and considering the corresponding damping and noise terms, and further applying the standard linearization procedure, we obtain the linearized quantum Langevin equations (QLEs),

$$\dot{b} = -i\tilde{\omega}_m b - 2i\Lambda b^\dagger + ig(c + c^\dagger) - \frac{\gamma_m}{2}b + \sqrt{\gamma_m}b_{\text{in}}(t),$$
$$\dot{c} = -i\Delta_c c + ig(b + b^\dagger) + 2Ge^{i\theta}c^\dagger e^{-2i\tilde{\omega}_m t}$$
$$\quad - \kappa c + \sqrt{2\kappa}c_{\text{in}}(t), \tag{3}$$

where

$$\Delta_c = \delta_c - 2g_0\beta, \qquad \tilde{\omega}_m = \omega_m + 2\Lambda,$$
$$\Lambda = 3\eta(4\beta^2 + 1), \qquad g = g_0|\alpha|. \tag{4}$$

Here b_{in} is the boson annihilation operator of the thermal noise with zero mean value whose nonzero correlation functions are

$$\langle b_{\text{in}}^\dagger(t)b_{\text{in}}(t')\rangle = n_m^{\text{th}}\delta(t - t'),$$
$$\langle b_{\text{in}}(t)b_{\text{in}}^\dagger(t')\rangle = (n_m^{\text{th}} + 1)\delta(t - t'), \tag{5}$$

where $n_m^{\text{th}} = [\exp(\hbar\omega_m/k_B T) - 1]^{-1}$ is the mean bath phonon number, and k_B is the Boltzmann constant. Moreover, c_{in} is the zero-mean cavity vacuum input noise operator with correlation functions

$$\langle c_{\text{in}}^\dagger(t)c_{\text{in}}(t')\rangle = n_c^{\text{th}}\delta(t - t'),$$
$$\langle c_{\text{in}}(t)c_{\text{in}}^\dagger(t')\rangle = (n_c^{\text{th}} + 1)\delta(t - t'), \tag{6}$$

where $n_c^{\text{th}} = [\exp(\hbar\omega_c/k_B T) - 1]^{-1}$ is the mean thermal excitation number of the optical mode.

The corresponding linearized system Hamiltonian can be written as

$$H_{\text{eff}} = \tilde{\omega}_m b^\dagger b + \Delta_c c^\dagger c + \Lambda(b^2 + b^{\dagger 2}) - g(b + b^\dagger)(c + c^\dagger)$$
$$\quad + iG(e^{i\theta}c^{\dagger 2}e^{-2i\tilde{\omega}_m t} - e^{-i\theta}c^2 e^{2i\tilde{\omega}_m t}). \tag{7}$$

We notice that in Eq. (7), the mechanical mode and cavity mode will be simultaneously squeezed under the action of Duffing nonlinearity and parametric pump driving, respectively. Then, a fantastically interesting problem is whether the squeezing of the cavity mode can be further transferred into the squeezed mechanical mode by properly choosing $\tilde{\omega}_m'$. If so, as shown in Fig. 2, the strong mechanical squeezing is achievable based on the joint effect between Duffing nonlinearity and parametric pump driving.
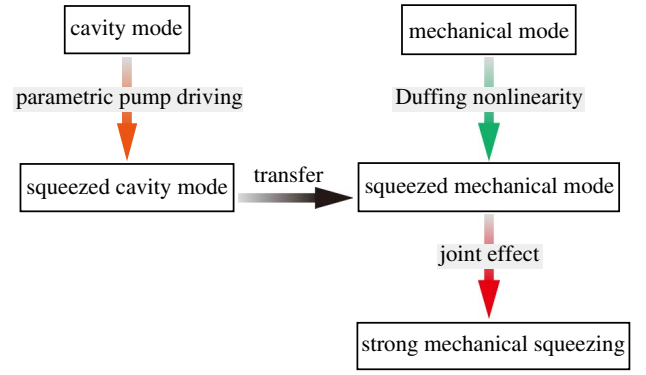
Fig. 2. Sketch of the physical processes of the joint effect between Duffing nonlinearity and parametric pump driving in construction of strong mechanical squeezing.

3. STEADY-STATE QUANTUM FLUCTUATION SPECTRA OF THE MECHANICAL MODE

If we apply the squeezing transformation $S(r) = \exp[\frac{r}{2}(b^2 - b^{\dagger 2})]$ with squeezing parameter

$$r = \frac{1}{4}\ln\left(1 + \frac{4\Lambda}{\omega_m}\right) \tag{8}$$

to the linearized Hamiltonian in Eq. (7), the system Hamiltonian can be transformed to be

$$H_{\text{eff}}' = S^\dagger(r)H_{\text{eff}}S(r)$$
$$= \tilde{\omega}_m' b^\dagger b + \Delta_c c^\dagger c - g'(b + b^\dagger)(c + c^\dagger)$$
$$\quad + iG(e^{i\theta}c^{\dagger 2}e^{-2i\tilde{\omega}_m' t} - e^{-i\theta}c^2 e^{2i\tilde{\omega}_m' t}), \tag{9}$$

where

$$\tilde{\omega}_m' = \sqrt{\omega_m^2 + 4\omega_m\Lambda}, \qquad g' = g\left(1 + \frac{4\Lambda}{\omega_m}\right)^{-\frac{1}{4}}. \tag{10}$$

In the interaction picture with respect to the free parts $\tilde{\omega}_m' b^\dagger b + \Delta_c c^\dagger c$, H_{eff}' is further transformed to

$$H_{\text{eff}}'' = -g'[e^{-i(\Delta_c + \tilde{\omega}_m')t}bc + e^{-i(\Delta_c - \tilde{\omega}_m')t}b^\dagger c$$
$$\quad + e^{i(\Delta_c - \tilde{\omega}_m')t}c^\dagger b + e^{i(\Delta_c + \tilde{\omega}_m')t}c^\dagger b^\dagger]$$
$$\quad + iG[e^{i\theta}c^{\dagger 2}e^{2i(\Delta_c - \tilde{\omega}_m')t} - e^{-i\theta}c^2 e^{-2i(\Delta_c - \tilde{\omega}_m')t}]. \tag{11}$$

We assume that $\tilde{\omega}_m' = \Delta_c$ and $\tilde{\omega}_m' \gg g'$ are satisfied. Under these parameter regimes, the rotating wave approximation can be made so that the fast oscillating terms $e^{\pm 2i\tilde{\omega}_m' t}$ in Eq. (11) can be safely ignored. Thus, H_{eff}'' can be simplified as

$$H_{\text{eff}}'' = -g'(b^\dagger c + c^\dagger b) + iG(e^{i\theta}c^{\dagger 2} - e^{-i\theta}c^2). \tag{12}$$

Obviously, the effective optomechanical interaction between the cavity mode and mechanical mode is a beam splitter interaction in the squeezing transformation frame. Therefore, the squeezing transfer from the squeezed cavity mode to the squeezed mechanical mode is possible.

A. Stability of the System

In this subsection, we begin to study the stability of the system by exploiting the Routh–Hurwitz criterion [47]. In the squeezing transformation frame, we obtain the linearized QLEs for the mechanical and cavity modes,

$$\dot{b} = ig'c - \frac{\gamma_m}{2}b + \sqrt{\gamma_m}b_{in}(t),$$

$$\dot{c} = ig'b + 2Ge^{i\theta}c^\dagger - \kappa c + \sqrt{2\kappa}c_{in}(t). \qquad (13)$$

Introducing the position and momentum quadratures for the mechanical mode and the thermal noise,

$$\delta Q = (b + b^\dagger)/\sqrt{2}, \qquad \delta P = (b - b^\dagger)/\sqrt{2}i,$$

$$Q_{in} = (b_{in} + b_{in}^\dagger)/\sqrt{2}, \qquad P_{in} = (b_{in} - b_{in}^\dagger)/\sqrt{2}i, \qquad (14)$$

and the amplitude and phase quadratures for the cavity mode and input quantum noise,

$$\delta X = (c + c^\dagger)/\sqrt{2}, \qquad \delta Y = (c - c^\dagger)/\sqrt{2}i,$$

$$X_{in} = (c_{in} + c_{in}^\dagger)/\sqrt{2}, \qquad Y_{in} = (c_{in} - c_{in}^\dagger)/\sqrt{2}i, \qquad (15)$$

the linearized QLEs for the mechanical and cavity modes in Eq. (13) can be written in a compact form as

$$\dot{f}(t) = Mf(t) + n(t), \qquad (16)$$

where $f(t)$ and $n(t)$ are the column vectors for all quadratures and noises, respectively,

$$f(t) = [\delta Q, \delta P, \delta X, \delta Y]^T,$$

$$n(t) = [\sqrt{\gamma_m}Q_{in}, \sqrt{\gamma_m}P_{in}, \sqrt{2\kappa}X_{in}, \sqrt{2\kappa}Y_{in}]^T, \qquad (17)$$

and M is a 4×4 time-independent matrix,

$$M = \begin{bmatrix} -\frac{\gamma_m}{2} & 0 & 0 & -g' \\ 0 & -\frac{\gamma_m}{2} & g' & 0 \\ 0 & -g' & 2G\cos\theta - \kappa & 2G\sin\theta \\ g' & 0 & 2G\sin\theta & -(2G\cos\theta + \kappa) \end{bmatrix}. \qquad (18)$$

The stability is determined by the eigenvalues of the matrix M, and the following three nontrivial stability conditions on the system parameters can be derived by requiring that all of the eigenvalues have negative real parts,

$$2\kappa(\kappa^2 - 4G^2) + \frac{1}{4}\gamma_m^3 + (2\kappa + \gamma_m)(g'^2 + 2\kappa\gamma_m) > 0,$$

$$\gamma_m^2(\kappa^2 - 4G^2) + 4g'^2(g'^2 + \kappa\gamma_m) > 0,$$

$$2\kappa\gamma_m(\kappa^2 - 4G^2)^2 + [(2\kappa + \gamma_m)^2 g'^2 + (4\kappa + \gamma_m)\kappa\gamma_m^2]$$

$$\times (\kappa^2 - 4G^2) + \kappa\gamma_m(2\kappa + \gamma_m)\left[\kappa\gamma_m^2 + \left(2\kappa + \frac{3}{2}\gamma_m\right)g'^2\right]$$

$$+ \frac{\gamma_m^3}{4}\left[\frac{\kappa\gamma_m^2}{2} + (2\kappa + \gamma_m)g'^2\right] > 0. \qquad (19)$$

Clearly, only if $G < 0.5\kappa$, can all stability conditions above always be satisfied. On the other hand, due to the fact that the similarity transformation in Eq. (9) does not change the eigenvalues of a matrix, $G < 0.5\kappa$ can still ensure the system is stable in the original frame (before the squeezing transformation). We also note that the stability is independent of the phase θ.

B. Quantum Fluctuation Spectra of the Mechanical Mode

To investigate the joint effect between Duffing nonlinearity and parametric pump driving in engineering of strong mechanical squeezing, it is very necessary to obtain the quantum fluctuation spectra of the mechanical mode.

Taking the Fourier transform of both sides in Eq. (16) by using $f(t) = \frac{1}{2\pi}\int_{-\infty}^\infty f(\omega)e^{-i\omega t}d\omega$, the position and momentum fluctuations of the mechanical mode in the frequency domain are obtained,

$$\delta Q(\omega) = A_1(\omega)Q_{in}(\omega) + B_1(\omega)P_{in}(\omega)$$
$$+ E_1(\omega)X_{in}(\omega) + F_1(\omega)Y_{in}(\omega),$$

$$\delta P(\omega) = A_2(\omega)Q_{in}(\omega) + B_2(\omega)P_{in}(\omega)$$
$$+ E_2(\omega)X_{in}(\omega) + F_2(\omega)Y_{in}(\omega), \qquad (20)$$

where

$$A_1(\omega) = \frac{\sqrt{\gamma_m}}{d(\omega)}\{[u(\omega)^2 - 4G^2]\nu(\omega) + g'^2 u(\omega) + 2Gg'^2\cos\theta\},$$

$$B_1(\omega) = \frac{\sqrt{\gamma_m}}{d(\omega)}2Gg'^2\sin\theta,$$

$$E_1(\omega) = -\frac{\sqrt{2\kappa}}{d(\omega)}2Gg'\sin\theta\nu(\omega),$$

$$F_1(\omega) = \frac{\sqrt{2\kappa}}{d(\omega)}g'\{[2G\cos\theta - u(\omega)]\nu(\omega) - g'^2\},$$

$$A_2(\omega) = \frac{\sqrt{\gamma_m}}{d(\omega)}2Gg'^2\sin\theta,$$

$$B_2(\omega) = \frac{\sqrt{\gamma_m}}{d(\omega)}\{[u(\omega)\nu(\omega) + g'^2]u(\omega)$$
$$- 4G^2\nu(\omega) - 2Gg'^2\cos\theta\},$$

$$E_2(\omega) = \frac{\sqrt{2\kappa}}{d(\omega)}g'\{[2G\cos\theta + u(\omega)]\nu(\omega) + g'^2\},$$

$$F_2(\omega) = \frac{\sqrt{2\kappa}}{d(\omega)}2Gg'\sin\theta\nu(\omega), \qquad (21)$$

with $u(\omega) = \kappa - i\omega$, $\nu(\omega) = \frac{\gamma_m}{2} - i\omega$, and $d(\omega) = [u(\omega)\nu(\omega) + g'^2]^2 - 4G^2\nu(\omega)^2$. In Eq. (20), the first two terms in $\delta Q(\omega)$ and $\delta P(\omega)$ originate from the thermal noise, while the last two terms are from the vacuum radiation input noise. In the absence of the optomechanical coupling between the cavity mode and mechanical mode ($g_0 = 0$), the mechanical oscillator will make quantum Brownian motion due to the coupling to the environment, $\delta Q(\omega) = \frac{\sqrt{\gamma_m}}{\frac{\gamma_m}{2} - i\omega}Q_{in}$ and $\delta P(\omega) = \frac{\sqrt{\gamma_m}}{\frac{\gamma_m}{2} - i\omega}P_{in}$.

The spectra of the position and momentum fluctuations of the mechanical mode are defined by

$$2\pi S_Z(\omega)\delta(\omega + \Omega)$$

$$= \frac{1}{2}[\langle\delta Z(\omega)\delta Z(\Omega)\rangle + \langle\delta Z(\Omega)\delta Z(\omega)\rangle], \quad Z = Q, P. \qquad (22)$$

Resorting to the noise sources correlation functions in the frequency domain,

$$\langle Q_{\text{in}}(\omega) Q_{\text{in}}(\Omega) \rangle = \langle P_{\text{in}}(\omega) P_{\text{in}}(\Omega) \rangle = \left(n_m^{\text{th}} + \frac{1}{2} \right) 2\pi \delta(\omega + \Omega),$$

$$\langle Q_{\text{in}}(\omega) P_{\text{in}}(\Omega) \rangle = -\langle P_{\text{in}}(\omega) Q_{\text{in}}(\Omega) \rangle = i\pi \delta(\omega + \Omega),$$

$$\langle X_{\text{in}}(\omega) X_{\text{in}}(\Omega) \rangle = \langle Y_{\text{in}}(\omega) Y_{\text{in}}(\Omega) \rangle = \left(n_c^{\text{th}} + \frac{1}{2} \right) 2\pi \delta(\omega + \Omega),$$

$$\langle X_{\text{in}}(\omega) Y_{\text{in}}(\Omega) \rangle = -\langle Y_{\text{in}}(\omega) X_{\text{in}}(\Omega) \rangle = i\pi \delta(\omega + \Omega), \qquad \textbf{(23)}$$

we can obtain the spectra of the position and momentum fluctuations of the mechanical mode in the squeezing transformation frame,

$$S_Q(\omega) = [A_1(\omega) A_1(-\omega) + B_1(\omega) B_1(-\omega)] \left(n_m^{\text{th}} + \frac{1}{2} \right)$$
$$+ [E_1(\omega) E_1(-\omega) + F_1(\omega) F_1(-\omega)] \left(n_c^{\text{th}} + \frac{1}{2} \right),$$

$$S_P(\omega) = [A_2(\omega) A_2(-\omega) + B_2(\omega) B_2(-\omega)] \left(n_m^{\text{th}} + \frac{1}{2} \right)$$
$$+ [E_2(\omega) E_2(-\omega) + F_2(\omega) F_2(-\omega)] \left(n_c^{\text{th}} + \frac{1}{2} \right). \qquad \textbf{(24)}$$

In $S_Z(\omega)(Z = Q, P)$, the first term is the contribution of the thermal noise, while the second term is from the input vacuum noise contribution. The steady-state mean square fluctuations of the mechanical mode $\langle \delta Q^2 \rangle$ and $\langle \delta P^2 \rangle$ corresponding to the position and momentum, respectively, in the original frame are obtained by

$$\langle \delta Q^2 \rangle = \frac{e^{-2r}}{2\pi} \int_{-\infty}^{\infty} S_Q(\omega) \mathrm{d}\omega, \quad \langle \delta P^2 \rangle = \frac{e^{2r}}{2\pi} \int_{-\infty}^{\infty} S_P(\omega) \mathrm{d}\omega. \qquad \textbf{(25)}$$

In the absence of optomechanical coupling, we can calculate $\langle \delta Q^2 \rangle = e^{-2r}(n_m^{\text{th}} + \frac{1}{2})$ and $\langle \delta P^2 \rangle = e^{2r}(n_m^{\text{th}} + \frac{1}{2})$. In this case, the steady-state amplitude of the mechanical mode is sufficiently small so that $r \simeq 0$. Therefore, $\langle \delta Q^2 \rangle = \langle \delta P^2 \rangle = n_m^{\text{th}} + \frac{1}{2}$. For $T = 0$, i.e., the mechanical oscillator is in the ground state, $\langle \delta Q^2 \rangle = \langle \delta P^2 \rangle = \frac{1}{2}$. Because of $[Q, P] = i$, according to the Heisenberg uncertainty principle, if either $\langle \delta Q^2 \rangle$ or $\langle \delta P^2 \rangle$ is below $1/2$, the mechanical mode will be squeezed. The degree of the squeezing of the mechanical mode can also be expressed in terms of $-10 \log_{10} \frac{\langle \delta Z^2 \rangle}{\langle \delta Z^2 \rangle_{\text{vac}}}$ $(Z = Q, P)$ with $\langle \delta Q^2 \rangle_{\text{vac}} = \langle \delta P^2 \rangle_{\text{vac}} = \frac{1}{2}$ being the position and momentum variances of the ground state.

4. STRONG MECHANICAL SQUEEZING INDUCED BY DUFFING NONLINEARITY AND PARAMETRIC PUMP DRIVING

A. Squeezing Transfer from Squeezed Cavity Mode to Mechanical Mode without Duffing Nonlinearity

When there is no optomechanical interaction ($g_0 = 0$), the amplitude and phase fluctuations of the cavity mode in the frequency domain can be obtained from Eq. (16),

$$\delta X(\omega) = E_3(\omega) X_{\text{in}}(\omega) + F_3(\omega) Y_{\text{in}}(\omega),$$
$$\delta Y(\omega) = E_4(\omega) X_{\text{in}}(\omega) + F_4(\omega) Y_{\text{in}}(\omega), \qquad \textbf{(26)}$$

where

$$E_3(\omega) = -\frac{\sqrt{2\kappa}}{4G^2 - u(\omega)^2} [u(\omega) + 2G \cos \theta],$$

$$F_3(\omega) = -\frac{\sqrt{2\kappa}}{4G^2 - u(\omega)^2} 2G \sin \theta,$$

$$E_4(\omega) = -\frac{\sqrt{2\kappa}}{4G^2 - u(\omega)^2} 2G \sin \theta,$$

$$F_4(\omega) = -\frac{\sqrt{2\kappa}}{4G^2 - u(\omega)^2} [u(\omega) - 2G \cos \theta]. \qquad \textbf{(27)}$$

In the absence of the OPA, i.e., $G = 0$, $\delta X(\omega)$ and $\delta Y(\omega)$ can be further simplified as $\delta X(\omega) = \frac{\sqrt{2\kappa}}{\kappa - i\omega} X_{\text{in}}(\omega)$ and $\delta Y(\omega) = \frac{\sqrt{2\kappa}}{\kappa - i\omega} Y_{\text{in}}(\omega)$. Taking the similar method with Eq. (24), we obtain the spectra of the amplitude and phase fluctuations of the cavity mode,

$$S_X(\omega) = [E_3(\omega) E_3(-\omega) + F_3(\omega) F_3(-\omega)] \left(n_c^{\text{th}} + \frac{1}{2} \right),$$

$$S_Y(\omega) = [E_4(\omega) E_4(-\omega) + F_4(\omega) F_4(-\omega)] \left(n_c^{\text{th}} + \frac{1}{2} \right). \qquad \textbf{(28)}$$

When there is no OPA in the cavity, the spectra of the amplitude and phase fluctuations of the cavity mode are $S_X(\omega) = S_Y(\omega) = \frac{2\kappa}{\kappa^2 + \omega^2}(n_c^{\text{th}} + \frac{1}{2})$, which are the Lorentzian spectra with full width 2κ at half-maximum, and their peaks are located at $\omega = 0$. The steady-state mean square fluctuations of the cavity mode $\langle \delta X^2 \rangle$ and $\langle \delta Y^2 \rangle$ corresponding to the amplitude and phase, respectively, are obtained:

$$\langle \delta O^2 \rangle = \frac{1}{2\pi} \int_{-\infty}^{\infty} S_O(\omega) \mathrm{d}\omega, \qquad O = X, Y. \qquad \textbf{(29)}$$

In the case of $G = 0$, we can derive $\langle \delta X^2 \rangle = \langle \delta Y^2 \rangle = n_c^{\text{th}} + \frac{1}{2}$. If the cavity mode is in the vacuum state, $\langle \delta X^2 \rangle = \langle \delta Y^2 \rangle = \frac{1}{2}$. Similarly, due to $[X, Y] = i$, if $\langle \delta X^2 \rangle$ or $\langle \delta Y^2 \rangle$ is smaller than $\frac{1}{2}$ (larger than 0 dB), the cavity mode is in a squeezed state.

Through numerically integrating Eq. (29), the phase mean square fluctuation $\langle \delta Y^2 \rangle$ of the cavity mode as a function of the parametric gain G with different parametric phases θ is shown in Fig. 3(a). We note that, in the absence of the OPA, $\langle \delta Y^2 \rangle = 0$ dB; hence, the phase fluctuation of the cavity mode is not squeezed. However, once the OPA is introduced, $\langle \delta Y^2 \rangle > 0$ dB appears, except $\theta = \frac{1}{2}\pi$. Therefore, the cavity mode phase squeezing is achievable when an OPA is inside the cavity. The optimal squeezing occurs at $\theta = 0$, and it becomes stronger as the parametric gain G increases. Hereafter, we will fix the parametric phase $\theta = 0$ to investigate the joint effect between Duffing nonlinearity and parametric pump driving in engineering of strong mechanical squeezing.

In the case of $\eta = 0$, taking the same method to numerically solve Eq. (25), we plot the mechanical mode position mean square fluctuation $\langle \delta Q^2 \rangle$ as a function of the parametric gain G with different parametric phases θ in Fig. 3(b). Similarly, it is seen that $\langle \delta Q^2 \rangle = 0$ dB in the absence of the OPA, so there is no squeezing in the position fluctuation of the mechanical mode. In the presence of the OPA, $\langle \delta Q^2 \rangle$ can be larger than 0 dB, except $\theta = \frac{1}{2}\pi$. From Figs. 3(a) and 3(b), we find that the phase fluctuation of the cavity mode is equal to the position
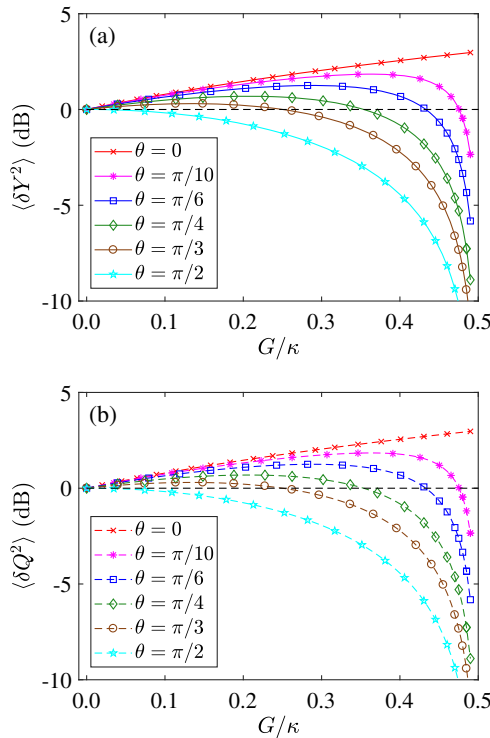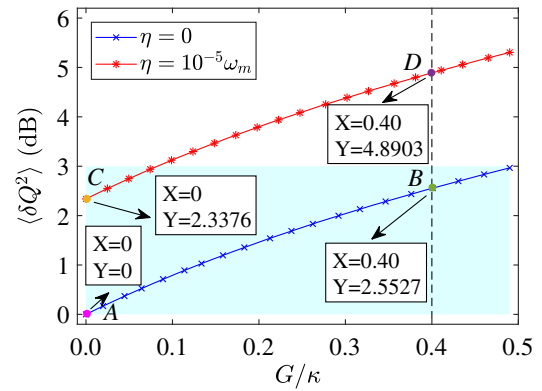
Fig. 3. Dependence of (a) the cavity mode phase mean square fluctuation $\langle\delta Y^2\rangle$ and (b) the mechanical mode position mean square fluctuation $\langle\delta Q^2\rangle$ on the parametric gain G for the parametric phase $\theta \in [0, \frac{1}{2}\pi]$. The horizontal dashed line represents the variance of the vacuum state. The frequency of the mechanical mode $\omega_m/(2\pi) = 2.5 \times 10^6$ Hz. Other parameters are $\omega_c = 2.5 \times 10^8 \omega_m$, $\gamma_m = 10^{-6}\omega_m$, $\kappa = 0.1\omega_m$, $g_0 = 10^{-4}\omega_m$, $P = 0.1$ mW, $n_m^{\text{th}} = n_c^{\text{th}} = 0$, and $\varepsilon_L = \sqrt{2P\kappa/(\hbar\omega_c)}$.

fluctuation of the mechanical mode for a fixed parameter set (G, θ). As a consequence, the squeezing of the cavity mode is completely transferred into the mechanical mode. This is because in the case of $\eta = 0$, the squeezing transformation $S(r)$ and the condition $\tilde{\omega}'_m = \Delta_c$ are reduced to an identity operator and the red-detuned driving regime $\omega_m = \Delta_c$, respectively. The effective optomechanical interaction between the cavity mode and the mechanical mode is a beam splitter-type interaction.

B. Strong Mechanical Squeezing Engineering Based on Joint Effect

In this subsection, we show the joint effect between Duffing nonlinearity and parametric pump driving in engineering of strong mechanical squeezing.

To this end, we plot the mechanical mode position mean square fluctuation $\langle\delta Q^2\rangle$ as a function of the parametric gain G without Duffing nonlinearity and with Duffing nonlinearity of $\eta = 10^{-5}\omega_m$, respectively, in Fig. 4. From Fig. 4, it is shown that, due to the limitation of the system stability ($G < 0.5\kappa$), the position squeezing of the mechanical mode cannot beat the 3 dB limit when there is only the parametric function (as the blue line shows). Likewise, when the weak nonlinearity of $\eta = 10^{-5}\omega_m$ is solely applied, the position squeezing cannot get beyond the 3 dB limit yet (as point C shows). However,

Fig. 4. Dependence of the mechanical mode position mean square fluctuation $\langle\delta Q^2\rangle$ on the parametric gain G in the cases of $\eta = 0$ and $\eta = 10^{-5}\omega_m$. The parameter sets (G, η) corresponding to the points A, B, C, and D are $(0, 0)$, $(0.4\kappa, 0)$, $(0, 10^{-5}\omega_m)$, and $(0.4\kappa, 10^{-5}\omega_m)$, respectively. Here we have set $\theta = 0$, and other parameters are the same as in Fig. 3. The shadowed blue bottom region corresponds to squeezing below the 3 dB limit.

once the parametric function and the weak nonlinearity simultaneously exist, the position squeezing of the mechanical mode can surpass the 3 dB limit (as the red line above the shadowed blue region shows). Therefore, based on the joint effect between Duffing nonlinearity and parametric pumping driving, the strong position squeezing that goes beyond the 3 dB limit can be engineered, but this cannot be achieved by only using either of these two manipulation methods.

Typically, in Fig. 4, we take four different points A, B, C, and D as an explicit example. The parameter sets (G, η) corresponding to the points A, B, C, and D are $(0, 0)$, $(0.4\kappa, 0)$, $(0, 10^{-5}\omega_m)$, and $(0.4\kappa, 10^{-5}\omega_m)$, respectively, which means four different cases: neither the Duffing nonlinearity and parametric pumping driving; only parametric pumping driving; only Duffing nonlinearity; and both of them. As shown in Fig. 4, the degrees of the squeezing ζ for A, B, C, and D are $\zeta_A = 0$ dB, $\zeta_B = 2.5527$ dB, $\zeta_C = 2.3376$ dB, and $\zeta_D = 4.8903$ dB, respectively. Obviously, $\zeta_D > 3$ dB $> \zeta_{B(C)}$, which explicitly demonstrates that the beyond 3 dB strong mechanical squeezing can easily be achieved from the joint effect of two different below 3 dB squeezing components induced by Duffing nonlinearity and parametric pump driving, respectively. In fact, $\zeta_D = \zeta_B + \zeta_C$. In next subsection, we will prove this analytically.

Intuitively, from the viewpoint of the Wigner function, this kind of joint squeezing effect between Duffing nonlinearity and parametric pump driving can be shown more clearly in the phase space. Since the thermal noise b_{in} and the vacuum input noise c_{in} are the zero-mean Gaussian noises, and the dynamics of the fluctuation operators b and c is linearized, the evolved state of the system will remain the Gaussian nature at all times [48]. Hence, the dynamics of the system can be completely characterized by a 4×4 covariance matrix (CM) σ, whose elements are defined by

$$\sigma_{ij} = \langle f_i(t)f_j(t) + f_j(t)f_i(t)\rangle/2, \qquad i, j = 1, 2, 3, 4.$$

$$(30)$$

Starting from the dynamical equation [Eq. (16)] for the quadrature fluctuation operators $f(t)$, we can derive the equation of motion for the CM σ [26],

$$\dot{\sigma}(t) = M\sigma(t) + \sigma(t)M^T + D, \tag{31}$$

where M^T represents the transpose of the matrix M, and D is a diffusion matrix whose elements are

$$D_{ij} = \langle n_i(t)n_j(t) + n_j(t)n_i(t)\rangle/2. \tag{32}$$

According to the noise correlation functions, it is found that D is a diagonal matrix $D = \mathrm{Diag}[\frac{\gamma_m}{2}(2n_m^{\mathrm{th}}+1), \frac{\gamma_m}{2}(2n_m^{\mathrm{th}}+1), \kappa(2n_c^{\mathrm{th}}+1), \kappa(2n_c^{\mathrm{th}}+1)]$. Note that Eq. (31) is an inhomogeneous first-order differential equation with 10 elements, which can be numerically solved with the initial condition $\sigma(0) = \mathrm{Diag}[e^{2r}(n_m^{\mathrm{th}}+\frac{1}{2}), e^{-2r}(n_m^{\mathrm{th}}+\frac{1}{2}), n_c^{\mathrm{th}}+\frac{1}{2}, n_c^{\mathrm{th}}+\frac{1}{2}]$.

When the system reaches steady state, the equation of motion for the CM σ [Eq. (31)] will be reduced as the Lyapunov equation,

$$M\sigma + \sigma M^T = -D. \tag{33}$$

If the 2×2 CM of the mechanical mode in the squeezing transformation frame σ_b can be written as

$$\sigma_b = \begin{bmatrix} \sigma_{b11} & \sigma_{b12} \\ \sigma_{b21} & \sigma_{b22} \end{bmatrix}, \tag{34}$$

the CM of the mechanical mode in the original frame is

$$\mathcal{V}_b = \begin{bmatrix} e^{-2r}\sigma_{b11} & \sigma_{b12} \\ \sigma_{b21} & e^{2r}\sigma_{b22} \end{bmatrix}. \tag{35}$$

In this case, the corresponding Wigner function of the mechanical mode can be written as [48]

$$W(\mathcal{R}) = \frac{\exp(-\frac{1}{2}\mathcal{R}^T\mathcal{V}_b^{-1}\mathcal{R})}{2\pi\sqrt{\mathrm{Det}[\mathcal{V}_b]}}, \tag{36}$$

where $\mathcal{R}$ stands for the two-dimensional vector of CM operators $\mathcal{R} = (Q, P)^T$.

In Fig. 5, we plot the Wigner functions in the phase space for the mechanical mode at some specific points in Fig. 4. Here we should point out that we have set the first moment of the mechanical mode to zero for simplicity. This is because the first moment could be arbitrarily adjusted by following a local unitary transformation, but it cannot affect any information-related properties [49,50]. It is shown in Fig. 5(a) that the Wigner function neither stretches nor contracts along any axis. It stems from the fact that at the point A in Fig. 4, there is neither parametric function nor Duffing nonlinearity, so the mechanical mode cannot be squeezed. As shown in Figs. 5(b) and 5(c), the Wigner function stretches along the vertical axis and contracts along the horizontal axis as a result of the Heisenberg uncertainty, which represents the squeezing effect of the position fluctuation under the sole action of parametric function (point B in Fig. 4) or Duffing nonlinearity (point C in Fig. 4), respectively. Obviously, these features of stretch and contraction of the Wigner function become more prominent in Fig. 5(d), which clearly signify the joint squeezing effect between Duffing nonlinearity and parametric pump driving at point D in Fig. 4.
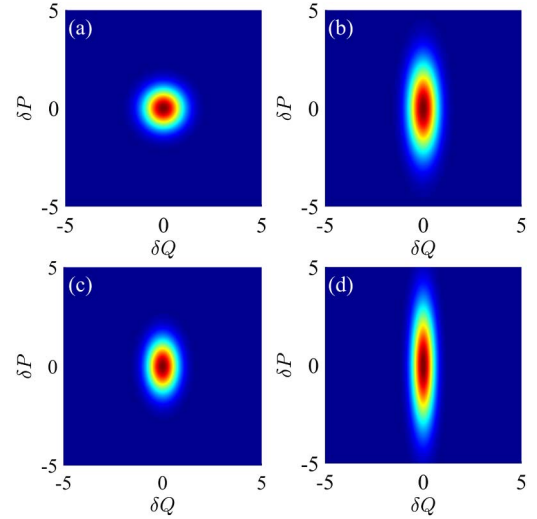
Fig. 5. Wigner function in the phase space for the mechanical mode. (a), (b), (c), and (d) correspond to the points A, B, C, and D in Fig. 4, respectively. The parameters are the same as in Fig. 4.

C. Understanding the Joint Effect from the Analytical Expression of the Mean Square Fluctuation

In this subsection, we provide the analytical approach to further understand the joint squeezing effect between Duffing nonlinearity and parametric pump driving.

Under the weak optomechanical coupling regime ($g' < \kappa$), the decay of the cavity mode is faster than that for the effective optomechanical coupling between the cavity mode and the mechanical mode, so that the cavity mode adiabatically interacts with the mechanical mode. Thus,

$$c = \frac{1}{\kappa^2 - 4G^2}[i\kappa g'b - 2iGg'e^{i\theta}b^\dagger \\ + 2Ge^{i\theta}\sqrt{2\kappa}c_{\mathrm{in}}^\dagger(t) + \kappa\sqrt{2\kappa}c_{\mathrm{in}}(t)]. \tag{37}$$

Substituting the above equation into Eq. (13), we have

$$\dot{b} = -\frac{\kappa g'^2}{\kappa^2 - 4G^2}b + \frac{2Gg'^2e^{i\theta}}{\kappa^2 - 4G^2}b^\dagger + \sqrt{\gamma_m}b_{\mathrm{in}}(t) \\ + \frac{ig'\sqrt{2\kappa}}{\kappa^2 - 4G^2}[2Ge^{i\theta}c_{\mathrm{in}}^\dagger(t) + \kappa c_{\mathrm{in}}(t)], \tag{38}$$
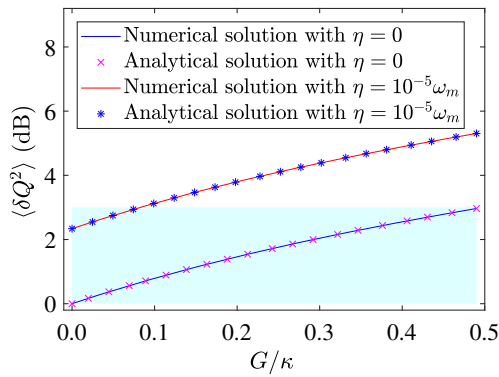
where the γ_m-dependent term in the coefficient of b has been ignored. The dynamical equation for the position fluctuation δQ can be derived:

$$\delta\dot{Q} = -\frac{g'^2}{\kappa + 2G}\delta Q + \mathcal{F}_1(t) + \mathcal{F}_2(t), \tag{39}$$

where

$$\mathcal{F}_1(t) = -\frac{ig'\sqrt{\kappa}}{\kappa + 2G}[c_{\mathrm{in}}^\dagger(t) - c_{\mathrm{in}}(t)],$$

$$\mathcal{F}_2(t) = \sqrt{\frac{\gamma_m}{2}}[b_{\mathrm{in}}^\dagger(t) + b_{\mathrm{in}}(t)], \tag{40}$$

are the effective Langevin forces, and their correlation functions are

Fig. 6. Mechanical mode position mean square fluctuation $\langle \delta Q^2 \rangle$ obtained by the numerical solution in Eq. (25) and the analytical solution in Eq. (44), respectively, in the cases of $\eta = 0$ and $\eta = 10^{-5} \omega_m$. Other parameters are the same as in Fig. 4. The shadowed blue bottom region corresponds to squeezing below the 3 dB limit.

$$\langle \mathcal{F}_1(t_1)\mathcal{F}_1(t_2) \rangle = \frac{g'^2 \kappa}{(\kappa + 2G)^2}(2n_c^{th} + 1)\delta(t_1 - t_2),$$

$$\langle \mathcal{F}_2(t_1)\mathcal{F}_2(t_2) \rangle = \frac{\gamma_m}{2}(2n_m^{th} + 1)\delta(t_1 - t_2). \quad \text{(41)}$$

From Eqs. (39) and (41), we can obtain the dynamical equation for the position mean square fluctuation $\langle \delta Q^2(t) \rangle$:

$$\frac{d\langle \delta Q^2(t) \rangle}{dt} = -\frac{2g'^2}{\kappa + 2G}\langle \delta Q^2(t) \rangle + \frac{g'^2 \kappa}{(\kappa + 2G)^2}(2n_c^{th} + 1)$$

$$+ \frac{\gamma_m}{2}(2n_m^{th} + 1). \quad \text{(42)}$$

Therefore, the analytical expression for the steady-state position mean square fluctuation $\langle \delta Q^2 \rangle$ in the original frame is

$$\langle \delta Q^2 \rangle_s = e^{-2r}\left[\frac{\kappa}{2(\kappa + 2G)}(2n_c^{th} + 1)\right.$$

$$\left. + \frac{\gamma_m(\kappa + 2G)}{4g'^2}(2n_m^{th} + 1)\right]. \quad \text{(43)}$$

If the degree of the squeezing of the steady-state position fluctuation is expressed in decibel units,

$$\zeta = -10 \log_{10}\frac{\langle \delta Q^2 \rangle_s}{\langle \delta Q^2 \rangle_{vac}}$$

$$= -10 \log_{10}e^{-2r} - 10 \log_{10}\left[\frac{\kappa}{2(\kappa + 2G)}\right.$$

$$\left. + \frac{\gamma_m(\kappa + 2G)}{4g'^2}\right] - 10 \log_{10}2, \quad \text{(44)}$$

we have set $n_c^{th} = n_m^{th} = 0$. Obviously, in Eq. (44), the first term is from the η-dependent squeezing contribution, while the second term is from the G-dependent squeezing contribution. The joint squeezing effect between Duffing nonlinearity and parametric pump driving just is the superposition of each kind of squeezing effect. This is the reason why $\zeta_D = \zeta_B + \zeta_C$ in Fig. 4. To verify the validity of Eq. (44), the analytical solution is also shown in Fig. 6. It can be seen that it agrees well with the exact numerical solution obtained by Eq. (25). In Table 1, we give the sole (joint) squeezing result of the parametric pump driving and the Duffing nonlinearity when applying either (both) of these two different squeezing methods in different parameter sets of (P, G, η). It proves again that the joint squeezing effect just corresponds to the superposition of their sole squeezing result.

In order to further show the robustness of the joint mechanical squeezing, we plot the mechanical mode position mean square fluctuation $\langle \delta Q^2 \rangle$ as a function of the thermal phonon number n_m^{th} in Fig. 7. We find that, even though the thermal phonon number n_m^{th} is about 10^5, the mechanical squeezing still can beat the 3 dB limit. It is also seen that the position squeezing of the mechanical mode decreases with the increase of the thermal phonon number n_m^{th}, which can be explained by Eq. (43), where $\langle \delta Q^2 \rangle$ increases with the n_m^{th}, i.e., the decrease of the position squeezing.

## 5. MEASUREMENT OF THE JOINT MECHANICAL SQUEEZING VIA OUTPUT FIELD

We now turn to discuss the mechanical squeezing measurement resorting to the output field. According to the input-output relation of the cavity field $c_{out}(t) = \sqrt{2\kappa}c(t) - c_{in}(t)$ [51], we can obtain the quadrature fluctuation of the output field in the frequency domain $\delta Z_{out}(\omega)(Z = X, Y)$. Here we define the quadrature fluctuation operator of the output field as

Table 1. Applying Either (Both) of the Parametric Pump Driving and the Duffing Nonlinearity, the Sole (Joint) Squeezing Result (in Units of Decibels) of These Two Different Squeezing Methods in Different Parameter Sets of $(P, G, \eta)^a$

Power P (mW)	Parametric Gain G/κ	Nonlinearity η/ω_m	Squeezing Effect ($G \neq 0$, $\eta = 0$)	Squeezing Effect ($G = 0$, $\eta \neq 0$)	Superposition	Joint Squeezing Effect ($G \neq 0$, $\eta \neq 0$)
0.1	0.30	10^{-5}	2.0412	2.3376	4.3788	4.3788
0.1	0.30	10^{-4}	2.0412	3.4081	5.4493	5.4492
0.5	0.35	10^{-5}	2.3045	3.8333	6.1378	6.1378
0.5	0.35	10^{-4}	2.3045	4.8904	7.1949	7.1948
1.0	0.40	10^{-5}	2.5527	4.4718	7.0245	7.0245
1.0	0.40	10^{-4}	2.5527	5.5188	8.0715	8.0715
2.0	0.45	10^{-5}	2.7875	5.1042	7.8917	7.8917
2.0	0.45	10^{-4}	2.7875	6.1419	8.9294	8.9294

^{a}Other parameters are the same as in Fig. 3.
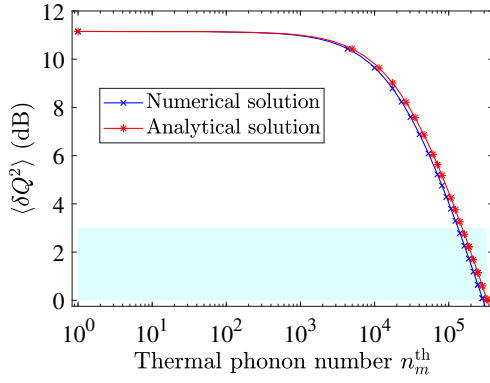
Fig. 7. Dependence of the mechanical mode position mean square fluctuation $\langle \delta Q^2 \rangle$ on the thermal phonon number n_m^{th}. Here we have set $\kappa = 0.2\omega_m$, $\eta = 10^{-4}\omega_m$, $G = 0.49\kappa$, $\theta = 0$, and $P = 10$ mW. Other parameters are the same as in Fig. 3. The shadowed blue bottom region corresponds to squeezing below the 3 dB limit.

$$\delta Z_{\text{out}}(\omega) = \frac{1}{\sqrt{2}}[\delta c_{\text{out}}(\omega)e^{-i\phi} + \delta c_{\text{out}}(-\omega)^\dagger e^{i\phi}], \quad (45)$$

where ϕ is the measurement phase angle in the homodyne measurement. When $\phi = 0$, $\delta Z_{\text{out}}(\omega) = \delta X_{\text{out}}(\omega)$, which corresponds to the amplitude fluctuation operator of the output field. While $\phi = \frac{\pi}{2}$, $\delta Z_{\text{out}}(\omega) = \delta Y_{\text{out}}(\omega)$, which is the phase fluctuation operator of the output field. $\delta Z_{\text{out}}(\omega)$ can be expanded in the following form:

$$\delta Z_{\text{out}}(\omega) = A_Z(\omega)Q_{\text{in}}(\omega) + B_Z(\omega)P_{\text{in}}(\omega)$$
$$+ E_Z(\omega)X_{\text{in}}(\omega) + F_Z(\omega)Y_{\text{in}}(\omega), \quad (46)$$

where

$$A_Z(\omega) = -\sqrt{\gamma_m}[\cos\phi E_1(\omega) + \sin\phi F_1(\omega)],$$
$$B_Z(\omega) = -\sqrt{\gamma_m}[\cos\phi E_2(\omega) + \sin\phi F_2(\omega)],$$
$$E_Z(\omega) = \cos\phi H(\omega) + \sin\phi I(\omega),$$
$$F_Z(\omega) = \cos\phi I(\omega) + \sin\phi R(\omega),$$
$$H(\omega) = \frac{2\kappa}{d(\omega)}\nu(\omega)\{g'^2 + [u(\omega) + 2G\cos\theta]\nu(\omega)\} - 1,$$
$$R(\omega) = \frac{2\kappa}{d(\omega)}\nu(\omega)\{g'^2 + [u(\omega) - 2G\cos\theta]\nu(\omega)\} - 1,$$
$$I(\omega) = \frac{4\kappa}{d(\omega)}G\sin\theta\nu(\omega)^2. \quad (47)$$

We define the spectrum of the quadrature fluctuation $\delta Z_{\text{out}}(\omega)$ of the output field as

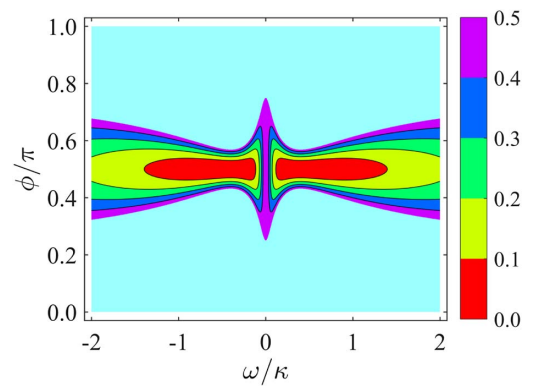$$2\pi S_{Z\text{out}}(\omega)\delta(\omega + \Omega)$$
$$= \frac{1}{2}[\langle \delta Z_{\text{out}}(\omega)\delta Z_{\text{out}}(\Omega)\rangle + \langle \delta Z_{\text{out}}(\Omega)\delta Z_{\text{out}}(\omega)\rangle]. \quad (48)$$

Using the correlations of the noise operators in the frequency domain in Eq. (23), we obtain the spectrum of the quadrature fluctuation $\delta Z_{\text{out}}(\omega)$ of the output field,

$$S_{Z\text{out}}(\omega) = [A_Z(\omega)A_Z(-\omega) + B_Z(\omega)B_Z(-\omega)]\left(n_m^{\text{th}} + \frac{1}{2}\right)$$
$$+ [E_Z(\omega)E_Z(-\omega) + F_Z(\omega)F_Z(-\omega)]\left(n_c^{\text{th}} + \frac{1}{2}\right). \quad (49)$$

In Eq. (49), the first term originates from the thermal noise, while the second term is from the vacuum input noise.

As discussed above, in this joint scheme, the two critical elements to engineer the strong mechanical squeezing are, respectively, parametric pump driving and mechanical Duffing nonlinearity. If neither of these two elements is introduced into optomechanical system ($G = 0$, $\eta = 0$) and there is no optomechanical coupling ($g_0 = 0$), the mechanical mode cannot be squeezed, and the spectra of the amplitude and phase fluctuations of the output field are $S_{X\text{out}}(\omega) = S_{Y\text{out}}(\omega) = \frac{1}{2}$, which means that the output field is in a vacuum state. In the presence of the optomechanical coupling ($g_0 \neq 0$), as shown in Fig. 8, we give the contour plot of the detection spectrum $S_{Z\text{out}}(\omega)$ of the quadrature fluctuation of the output field versus the frequency ω and the measurement phase angle ϕ when $G = 0.4\kappa$ and $\eta = 10^{-5}\omega_m$. Figure 8 clearly presents the region where the detection spectrum $S_{Z\text{out}}(\omega)$ of the quadrature fluctuation $\delta Z_{\text{out}}(\omega)$ of the output field is squeezed, i.e., $S_{Z\text{out}}(\omega) < \frac{1}{2}$. In other words, once the parametric pump driving and mechanical Duffing nonlinearity are applied to an optomechanical system to engineer the strong mechanical squeezing, the spectrum $S_{Z\text{out}}(\omega)$ of the quadrature fluctuation of the output field can be turned into a squeezed state from the previous vacuum state when the phase angle ϕ is appropriate. In this sense, the quadrature squeezing of the output field is a vital signature of the mechanical squeezing constructed by the joint effect between parametric pump driving and Duffing nonlinearity. Therefore, the joint effect-induced strong mechanical squeezing can be directly detected by measuring the quadrature fluctuation of the output field via the homodyne technology.

Fig. 8. Contour plot of the detection spectrum $S_{Z\text{out}}(\omega)$ of the quadrature fluctuation of the output field versus the frequency ω and the measurement phase angle ϕ when $G = 0.4\kappa$ and $\eta = 10^{-5}\omega_m$. Other parameters are the same as in Fig. 4.

6. ANALYSES OF THE EXPERIMENTAL FEASIBILITY

Before concluding, we give some analyses of the experimental feasibility of the present scheme. Based on the current experimental setups of optomechanical systems, the order of magnitude for the system parameters extracted in our scheme is in the reasonable range. The joint strong mechanical squeezing effect in the present scheme results from two key factors, i.e., the parametric pump driving and the Duffing nonlinearity. The parametric pump driving of the OPA was one of the earliest candidates to produce the squeezed cavity field in experiment [11] and has been a mature technology so far, while the generation of Duffing nonlinearity has been discussed in detail in Refs. [36,46]. Moreover, we also note that the very large nonlinearity can be induced for the librational mode in levitated optomechanics [52]. In addition, the measurement of the joint mechanical squeezing can be directly performed by the homodyne detection technology using a local oscillator with an appropriate phase.

7. CONCLUSIONS

In conclusion, we have in detail discussed that the beyond 3 dB strong mechanical squeezing can be engineered successfully based on the joint effect between Duffing nonlinearity and parametric pump driving without the need of any extra technologies, such as quantum measurement or quantum feedback. We find that the reasonable choice of the parametric pump frequency can modulate the effective optomechanical interaction between cavity mode and mechanical mode as a beam splitter-type interaction in the squeezing transformation frame, which means that the squeezing of the cavity mode created by the OPA inside the optomechanical cavity can be further transferred into the squeezed mechanical mode induced by the Duffing nonlinearity. Resorting to this kind of joint effect, the 3 dB limit of strong mechanical squeezing can be easily beaten, but the two respective independent squeezing components are permitted below 3 dB. Particularly, we have numerically and analytically demonstrated that, as to the ideal mechanical bath, the joint mechanical squeezing effect just is the superposition of these two respective independent squeezing components. Moreover, the mechanical squeezing constructed by the joint effect has fairly strong robustness against mechanical thermal noise. Even though the thermal phonon number is about 10^5, the mechanical squeezing still can beat the 3 dB limit. We also show that the measurement of the joint mechanical squeezing can be directly performed via measuring the squeezing of the quadrature fluctuation of the output field by the homodyne detection technology without the need of introducing an additional ancillary cavity mode. The joint idea provides an alternative approach to engineer strong mechanical squeezing and can also be generalized to realize other strong macroscopic quantum effects.

REFERENCES

1. M. O. Scully and M. S. Zubairy, Quantum Optics (Cambridge University, 1997).
2. C. M. Caves, K. S. Thorne, R. W. P. Drever, V. D. Sandberg, and M. Zimmermann, "On the measurement of a weak classical force coupled to a quantum-mechanical oscillator. I. Issues of principle," Rev. Mod. Phys. 52, 341–392 (1980).
3. A. Abramovici, W. E. Althouse, R. W. P. Drever, Y. Gürsel, S. Kawamura, F. J. Raab, D. Shoemaker, L. Sievers, R. E. Spero, K. S. Thorne, R. E. Vogt, R. Weiss, S. E. Whitcomb, and M. E. Zucker, "LIGO: the laser interferometer gravitational-wave observatory," Science 256, 325–333 (1992).
4. M. D. LaHaye, O. Buu, B. Camarota, and K. C. Schwab, "Approaching the quantum limit of a nanomechanical resonator," Science 304, 74–77 (2004).
5. M. Aspelmeyer, P. Meystre, and K. Schwab, "Quantum optomechanics," Phys. Today 65, 29–35 (2012).
6. W. H. Zurek, "Decoherence and the transition from quantum to classical," Phys. Today 44, 36–44 (1991).
7. T. J. Kippenberg and K. J. Vahala, "Cavity optomechanics: back-action at the mesoscale," Science 321, 1172–1176 (2008).
8. S. L. Braunstein and P. van Loock, "Quantum information with continuous variables," Rev. Mod. Phys. 77, 513–577 (2005).
9. D. F. Walls, "Squeezed states of light," Nature 306, 141–146 (1983).
10. R. E. Slusher, L. W. Hollberg, B. Yurke, J. C. Mertz, and J. F. Valley, "Observation of squeezed states generated by four-wave mixing in an optical cavity," Phys. Rev. Lett. 55, 2409–2412 (1985).
11. L. A. Wu, H. J. Kimble, J. L. Hall, and H. Wu, "Generation of squeezed states by parametric down conversion," Phys. Rev. Lett. 57, 2520–2523 (1986).
12. J. N. Hollenhorst, "Quantum limits on resonant-mass gravitational-radiation detectors," Phys. Rev. D 19, 1669–1679 (1979).
13. H. Lü, Y. Jiang, Y. Z. Wang, and H. Jing, "Optomechanically induced transparency in a spinning resonator," Photon. Res. 5, 367–371 (2017).
14. S. Gigan, H. R. Böhm, M. Paternostro, F. Blaser, G. Langer, J. B. Hertzberg, K. C. Schwab, D. Bäuerle, M. Aspelmeyer, and A. Zeilinger, "Self-cooling of a micromirror by radiation pressure," Nature 444, 67–70 (2006).
15. T. Rocheleau, T. Ndukum, C. Macklin, J. B. Hertzberg, A. A. Clerk, and K. C. Schwab, "Preparation and detection of a mechanical resonator near the ground state of motion," Nature 463, 72–75 (2010).
16. J. D. Teufel, T. Donner, D. Li, J. W. Harlow, M. S. Allman, K. Cicak, A. J. Sirois, J. D. Whittaker, K. W. Lehnert, and R. W. Simmonds, "Sideband cooling of micromechanical motion to the quantum ground state," Nature 475, 359–363 (2011).
17. J. Chan, T. P. M. Alegre, A. H. Safavi-Naeini, J. T. Hill, A. Krause, S. Gröblacher, M. Aspelmeyer, and O. Painter, "Laser cooling of a nanomechanical oscillator into its quantum ground state," Nature 478, 89–92 (2011).
18. J. B. Clark, F. Lecocq, R. W. Simmonds, J. Aumentado, and J. D. Teufel, "Sideband cooling beyond the quantum backaction limit with squeezed light," Nature 541, 191–195 (2017).
19. J. D. Thompson, B. M. Zwickl, A. M. Jayich, F. Marquardt, S. M. Girvin, and J. G. E. Harris, "Strong dispersive coupling of a high-finesse cavity to a micromechanical membrane," Nature 452, 72–75 (2008).
20. S. Gröblacher, K. Hammerer, M. R. Vanner, and M. Aspelmeyer, "Observation of strong coupling between a micromechanical resonator and an optical cavity field," Nature 460, 724–727 (2009).
21. J. C. Sankey, C. Yang, B. M. Zwickl, A. M. Jayich, and J. G. E. Harris, "Strong and tunable nonlinear optomechanical coupling in a low-loss system," Nat. Phys. 6, 707–712 (2010).
22. M. Aspelmeyer, T. J. Kippenberg, and F. Marquardt, "Cavity optomechanics," Rev. Mod. Phys. 86, 1391–1452 (2014).
23. A. Mari and J. Eisert, "Gently modulating optomechanical systems," Phys. Rev. Lett. 103, 213603 (2009).

24. J. Q. Liao and C. K. Law, "Parametric generation of quadrature squeezing of mirrors in cavity optomechanics," Phys. Rev. A **83**, 033820 (2011).

25. M. Schmidt, M. Ludwig, and F. Marquardt, "Optomechanical circuits for nanomechanical continuous variable quantum state processing," New J. Phys. **14**, 125005 (2012).

26. C. H. Bai, D. Y. Wang, S. Zhang, S. Liu, and H. F. Wang, "Modulation-based atom-mirror entanglement and mechanical squeezing in an unresolved-sideband optomechanical system," Ann. Phys. **531**, 1800271 (2019).

27. M. J. Woolley, A. C. Doherty, G. J. Milburn, and K. C. Schwab, "Nanomechanical squeezing with detection via a microwave cavity," Phys. Rev. A **78**, 062303 (2008).

28. A. Kronwald, F. Marquardt, and A. A. Clerk, "Arbitrarily large steady-state bosonic squeezing via dissipation," Phys. Rev. A **88**, 063833 (2013).

29. R. Zhang, Y. Fang, Y. Y. Wang, S. Chesi, and Y. D. Wang, "Strong mechanical squeezing in an unresolved-sideband optomechanical system," Phys. Rev. A **99**, 043805 (2019).

30. K. Jähne, C. Genes, K. Hammerer, M. Wallquist, E. S. Polzik, and P. Zoller, "Cavity-assisted squeezing of a mechanical oscillator," Phys. Rev. A **79**, 063819 (2009).

31. A. Nunnenkamp, K. Børkje, J. G. E. Harris, and S. M. Girvin, "Cooling and squeezing via quadratic optomechanical coupling," Phys. Rev. A **82**, 021806 (2010).

32. M. Asjad, G. S. Agarwal, M. S. Kim, P. Tombesi, G. D. Giuseppe, and D. Vitali, "Robust stationary mechanical squeezing in a kicked quadratic optomechanical system," Phys. Rev. A **89**, 023849 (2014).

33. S. Huang and G. S. Agarwal, "Reactive coupling can beat the motional quantum limit of nanowaveguides coupled to a microdisk resonator," Phys. Rev. A **82**, 033811 (2010).

34. W. J. Gu, G. X. Li, and Y. P. Yang, "Generation of squeezed states in a movable mirror via dissipative optomechanical coupling," Phys. Rev. A **88**, 013835 (2013).

35. W. J. Gu and G. X. Li, "Squeezing of the mirror motion via periodic modulations in a dissipative optomechanical system," Opt. Express **21**, 20423–20440 (2013).

36. X. Y. Lü, J. Q. Liao, L. Tian, and F. Nori, "Steady-state mechanical squeezing in an optomechanical system via Duffing nonlinearity," Phys. Rev. A **91**, 013834 (2015).

37. B. Xiong, X. Li, S. L. Chao, and L. Zhou, "Optomechanical quadrature squeezing in the non-Markovian regime," Opt. Lett. **43**, 6053–6056 (2018).

38. A. A. Clerk, F. Marquardt, and K. Jacobs, "Back-action evasion and squeezing of a mechanical resonator using a cavity detector," New J. Phys. **10**, 095010 (2008).

39. A. Szorkovszky, A. C. Doherty, G. I. Harris, and W. P. Bowen, "Mechanical squeezing via parametric amplification and weak measurement," Phys. Rev. Lett. **107**, 213603 (2011).

40. A. Szorkovszky, G. A. Brawley, A. C. Doherty, and W. P. Bowen, "Strong thermomechanical squeezing via weak measurement," Phys. Rev. Lett. **110**, 184301 (2013).

41. R. Ruskov, K. Schwab, and A. N. Korotkov, "Squeezing of a nanomechanical resonator by quantum nondemolition measurement and feedback," Phys. Rev. B **71**, 235407 (2005).

42. A. Dalafi, M. H. Naderi, and A. Motazedifard, "Effects of quadratic coupling and squeezed vacuum injection in an optomechanical cavity assisted with a Bose-Einstein condensate," Phys. Rev. A **97**, 043619 (2018).

43. A. Farace and V. Giovannetti, "Enhancing quantum effects via periodic modulations in optomechanical systems," Phys. Rev. A **86**, 013820 (2012).

44. D. Y. Wang, C. H. Bai, S. Liu, S. Zhang, and H. F. Wang, "Optomechanical cooling beyond the quantum backaction limit with frequency modulation," Phys. Rev. A **98**, 023816 (2018).

45. J. F. Huang, J. Q. Liao, and L. M. Kuang, "Ultrastrong Jaynes-Cummings model," arXiv:1902.05779 (2019).

46. K. Jacobs and A. J. Landahl, "Engineering giant nonlinearities in quantum nanosystems," Phys. Rev. Lett. **103**, 067201 (2009).

47. E. X. DeJesus and C. Kaufman, "Routh-Hurwitz criterion in the examination of eigenvalues of a system of nonlinear ordinary differential equations," Phys. Rev. A **35**, 5288–5290 (1987).

48. C. Weedbrook, S. Pirandola, R. García-Patrón, N. J. Cerf, T. C. Ralph, J. H. Shapiro, and S. Lloyd, "Gaussian quantum information," Rev. Mod. Phys. **84**, 621–669 (2012).

49. R. X. Chen, L. T. Shen, Z. B. Yang, and H. Z. Wu, "Transition of entanglement dynamics in an oscillator system with weak time-dependent coupling," Phys. Rev. A **91**, 012312 (2015).

50. S. Chakraborty and A. K. Sarma, "Entanglement dynamics of two coupled mechanical oscillators in modulated optomechanics," Phys. Rev. A **97**, 022336 (2018).

51. D. F. Walls and G. J. Milburn, *Quantum Optics* (Springer-Verlag, 1994).

52. K. W. Xiao, N. Zhao, and Z. Q. Yin, "Bistability and squeezing of the librational mode of an optically trapped nanoparticle," Phys. Rev. A **96**, 013837 (2017).